SN 2022crr: A Nearby Broad-lined Type Ic Supernova

Muhammad Mousa, Gokul Srinivasaragavan, Maryam Modjaz, Brad Cenko

Abstract

We present photometric and spectroscopic observations of SN 2022crr, a nearby broad-lined Type Ic supernova (Ic-BL) discovered by the Zwicky Transient Facility. SN 2022crr exhibits high expansion velocities and a luminous light curve, consistent with other Type Ic-BL SNe. We analyze multi-band photometry to estimate key parameters within the system, including the progenitor mass. We compare its spectral evolution with those of other well-studied SNe Ic-BL. These observations contribute to the growing sample of Ic-BL supernovae, which are of particular interest due to their connection to long-duration gamma-ray bursts (LGRBs).

1 Introduction

Type Ic supernovae (SNe Ic) are core-collapse explosions of massive stars that have been stripped of both their hydrogen and helium envelopes. A subclass of these, the broad-lined SNe Ic (SNe Ic-BL), exhibit exceptionally high expansion velocities ($\gtrsim$ 15,000 km s^{-1}), which are inferred from the Doppler-broadened spectral lines. These events are of particular astrophysical interest due to their association with long-duration gamma-ray bursts (LGRBs).

The archetypal SN Ic-BL is SN 1998bw, which was spatially and temporally associated with GRB 980425 [**?**]. Since then, numerous other Ic-BL events have been discovered, some associated with GRBs (e.g., SN 2003dh, SN 2010bh) and many without. Whether all SNe Ic-BL harbor a central engine or only a subset is still an open question in the field.

SN 2022crr was discovered by the Zwicky Transient Facility (ZTF) on 2022 February 27.45 UT at a magnitude of $r \approx 18.3$ [**?**]. Its classification spectrum revealed a blue continuum with broad absorption features consistent with a young Type Ic-BL SN. Follow-up observations were initiated shortly after discovery, including multi-band photometry and low-resolution optical spectroscopy, including nebular spectroscopy.

In this work, we present a detailed analysis of SN 2022crr, focusing on its spectroscopic evolution and properties. We aim to place it in the context of the broader Ic-BL population and investigate the diversity of explosion parameters within this class.

2 Observations

2.1 Photometry

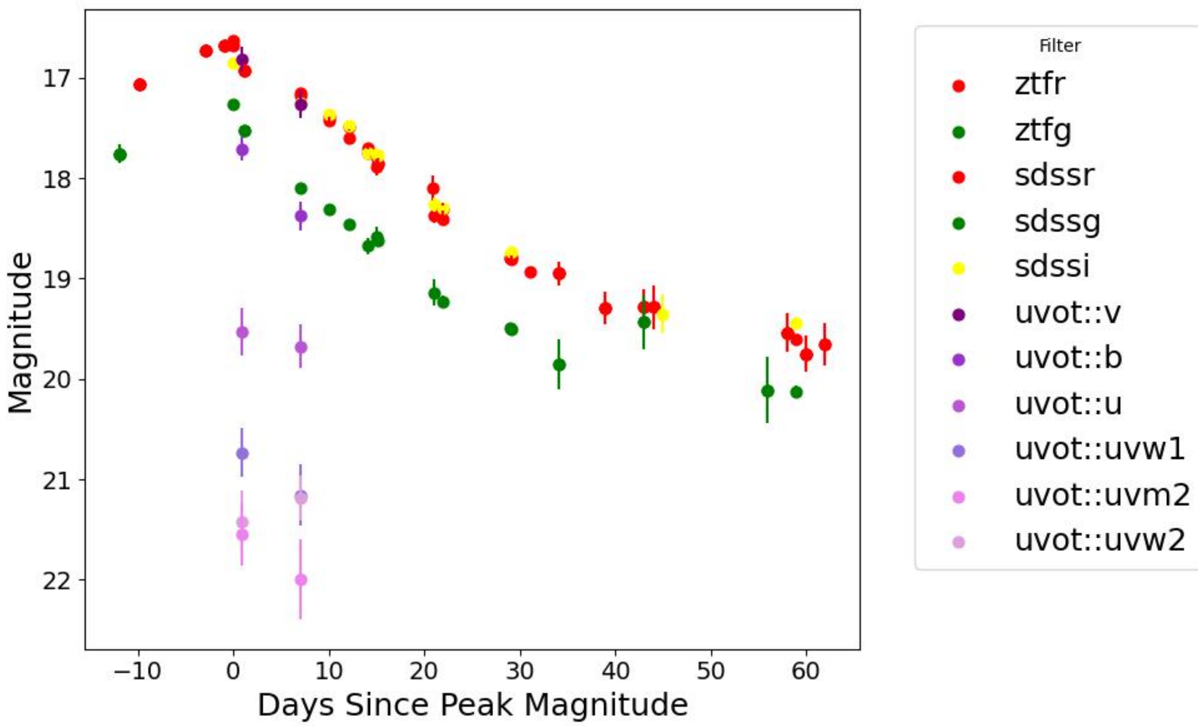

Figure 1: Multi-band light curve of SN 2022crr constructed using data from ZTF, SDSS, and Swift/UVOT.

We produced a multi-band photometric light curve of SN 2022crr using data from the Zwicky Transient Facility (ZTF), the Sloan Digital Sky Survey (SDSS), and the Swift UltraViolet and Optical Telescope (UVOT). The light curve includes filters from the optical (g, r, i) and ultraviolet (UVOT $uvw1$, $uvw2$, $uvm2$) bands. The transient exhibits a relatively sharp rise to peak, followed by a gradual decline in all bands, with the post-peak decline rate most pronounced in the bluer filters. This color evolution is consistent with a cooling photosphere and is characteristic of Type Ic-BL supernovae. The overall light curve morphology and luminosity are comparable to canonical SNe Ic-BL such as SN 2002ap and SN 2010ah.

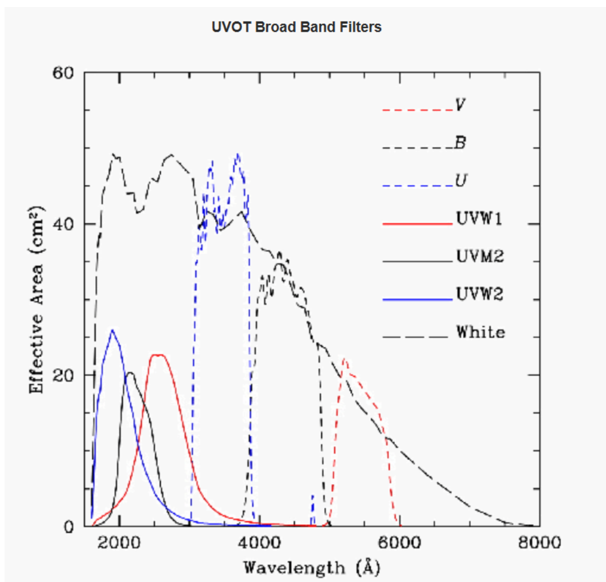

Figure 2: Effective area curves of the Swift/UVOT filters used in the photometric analysis of SN 2022crr.

2.2 Blackbody Fits and Radius/Temperature Evolution

To infer the thermal properties of SN 2022crr, we converted observed magnitudes to flux densities and performed blackbody fits to the spectral energy distribution at multiple epochs. This approximation is justified at early times when the ejecta are optically thick.

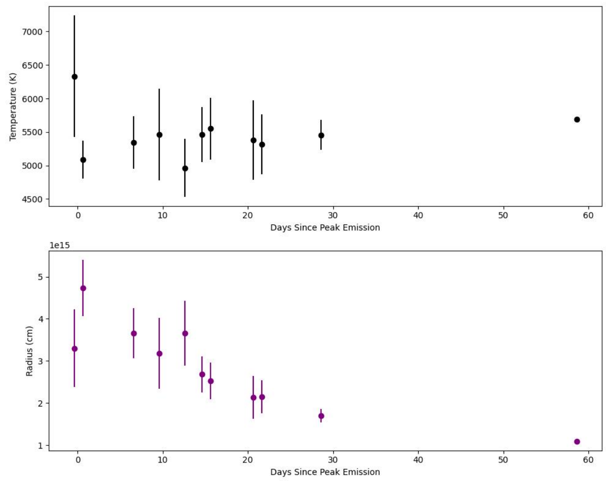

Figure 3: Temporal evolution of the blackbody-derived photospheric temperature (top) and radius (bottom) for SN 2022crr.

The temperature evolution is relatively stagnant, with values ranging from $\sim$ 5000 K to $\sim$ 6500 K over the first two months post-peak, suggesting persistent heating from radioactive decay and continued photon diffusion from the inner ejecta. In contrast, the photospheric radius exhibits a declining trend, decreasing from approximately 5×10^{15} cm to below 2×10^{15} cm over the same period. This behavior is consistent with the recession of the effective photosphere as the outer layers become more optically thin. The radius and temperature were computed using the relations:

$$F = \sigma T^4 \left(\frac{R}{D} \right)^2, \quad (1)$$

$$L = 4\pi R^2 \sigma T^4, \quad (2)$$

where F is the observed flux, T is the effective temperature, R is the radius of the emitting surface (photosphere), D is the distance to the supernova, and σ is the Stefan–Boltzmann constant.

2.3 Spectroscopy

Our spectroscopic campaign on SN 2022crr includes 17 spectra spanning from +12 to +133 days relative to estimated peak brightness. Spectra were obtained using SEDM, LRIS, and ALFOSC.

The early-time spectra are dominated by broad P-Cygni features indicative of high-velocity ejecta, with notable absorption from Fe II, O I, and Ca II. Line velocities exceed 20,000 km s^{-1} in early epochs, consistent with the broad-lined classification. As the SN transitions into the nebular phase, emission lines begin to dominate the spectra, and the continuum fades. The two latest spectra at +109 and +133 days reveal [O I] $\lambda\lambda$6300, 6364 and [Ca II] $\lambda\lambda$7291, 7324 emission lines, which provide constraints on the nucleosynthetic yields and the geometry of the inner ejecta.

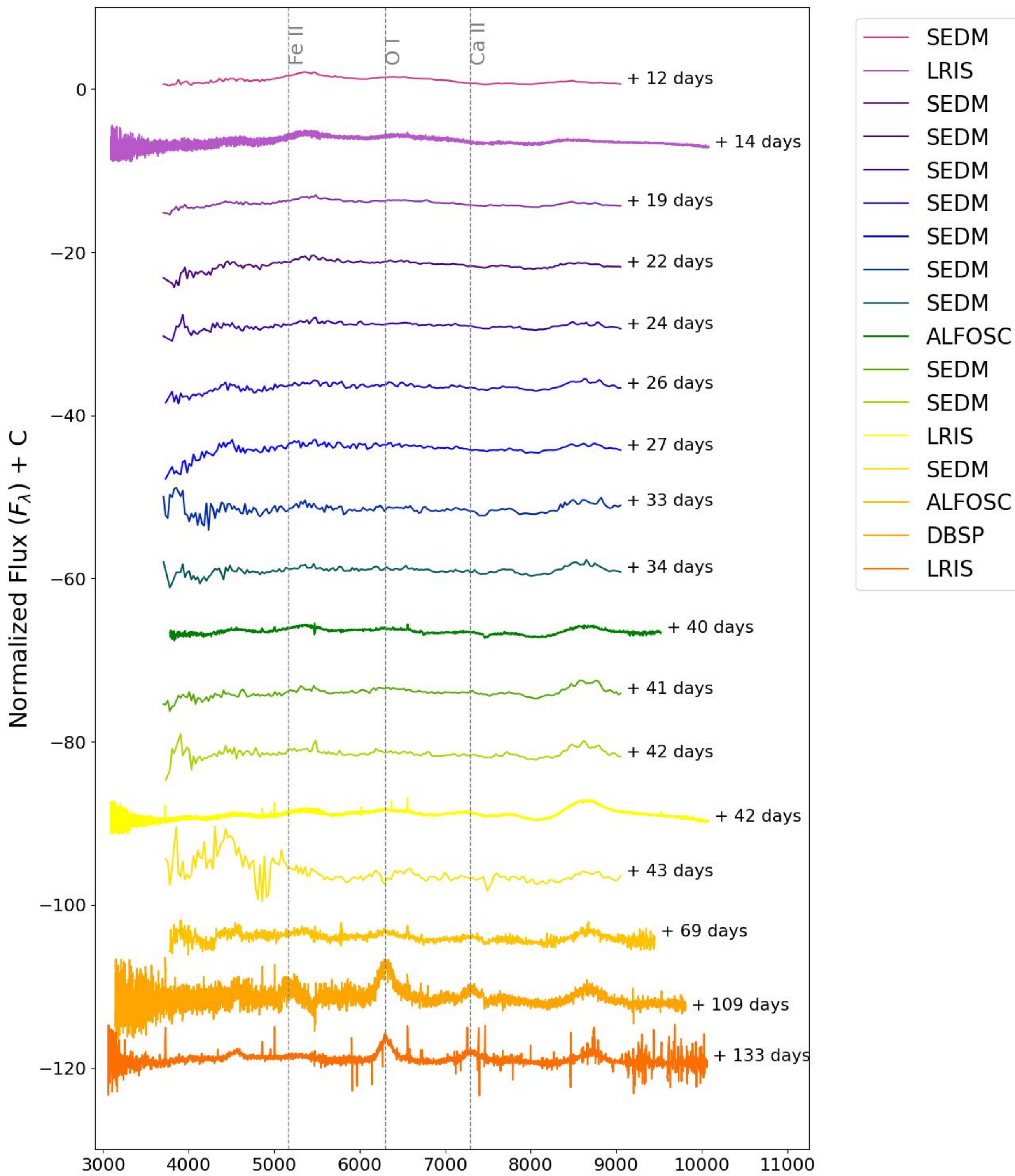

Figure 4: Spectral sequence of SN 2022crr from +12 to +133 days post-peak. Includes 15 photospheric spectra and 2 nebular spectra

2.4 Nebular Line Analysis and Progenitor Mass Constraints

In order to extract physical properties of the progenitor system, we further analyzed the two nebular-phase spectra obtained at +109 and +133 days post-peak. At these late epochs, the ejecta have expanded and become optically thin, allowing us to probe the inner regions where nucleosynthetic products dominate the emission. This makes nebular spectroscopy a powerful diagnostic for estimating the progenitor's core composition and initial mass.

We began by performing continuum subtraction on the flux-calibrated spectra using low-order polynomial fits to isolate prominent emission features. Particular attention was given to the [O I] $\lambda\lambda$6300, 6364 and [Ca II] $\lambda\lambda$7291, 7324 emission complexes, which are the dominant cooling lines during the nebular phase and serve as proxies for the oxygen and calcium mass in the ejecta.

Gaussian profiles were fit to each of the [O I] and [Ca II] features to quantify their integrated fluxes. These fits are shown on the DBSP spectrum in Figure 5. From these fits, we calculated the flux ratio of [O I]/[Ca II], which has been shown to correlate with the zero-age main sequence (ZAMS) mass of the progenitor star [Jerkstrand et al., 2015]. In general, higher-mass progenitors synthesize more oxygen relative to calcium, leading to larger [O I]/[Ca II] ratios.

For SN 2022crr, we find a line ratio of [O I]/[Ca II] = 2.93 from the DBSP spectrum at +109 days and 2.06 from the LRIS spectrum at +133 days. The discrepancy between epochs likely reflects changing ionization conditions and potential contamination by overlapping emission features, but both values are within the range observed for other SNe Ic-BL.

To contextualize these measurements, we compare our line ratios with a sample of well-studied Type Ib/c and Ic-BL supernovae from the literature. As shown in Figure 6, SN 2022crr occupies the higher end of the [O I]/[Ca II] distribution, suggestive of a relatively massive progenitor, consistent with expectations for a stripped-envelope supernova formed from a Wolf–Rayet star or a massive helium star in a close binary system.

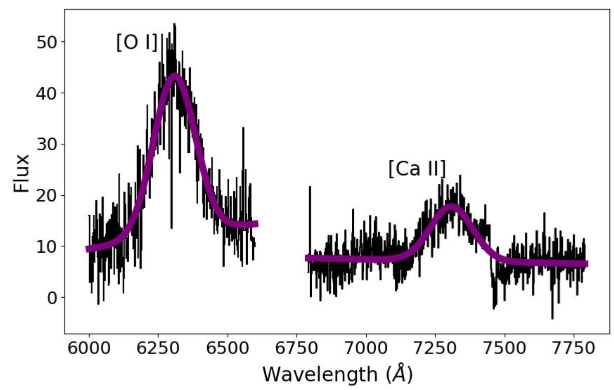

Figure 5: Gaussian fits to the [O I] and [Ca II] emission features from the DBSP spectrum at +109 days. The measured [O I]/[Ca II] line ratio is 2.93.

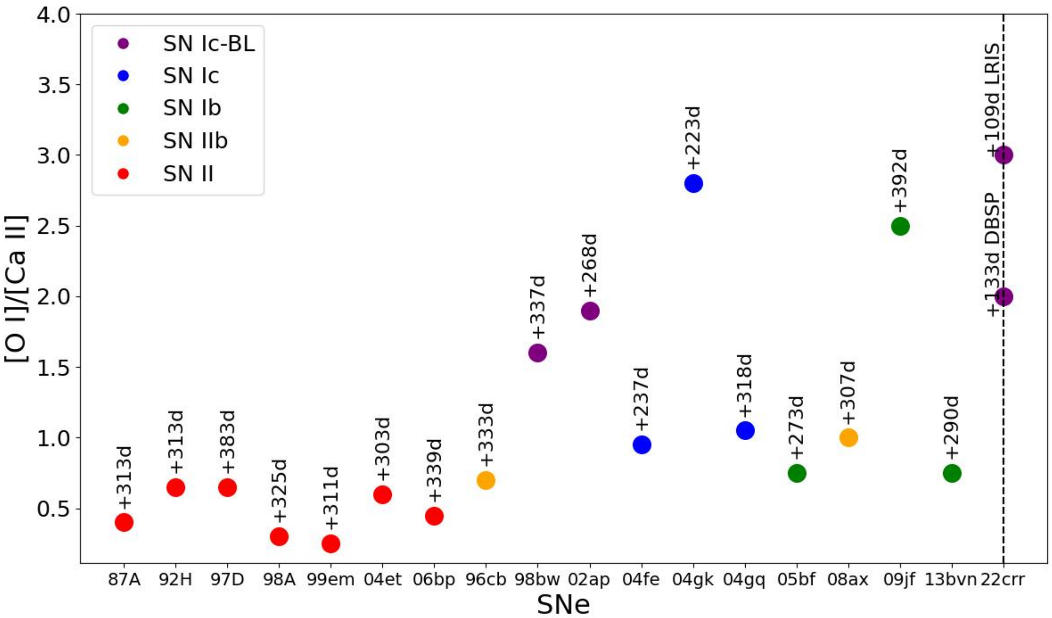

Figure 6: Comparison of [O I]/[Ca II] line ratios for SN 2022crr and other stripped-envelope SNe from the literature. SN 2022crr lies toward the upper end of the distribution, implying a relatively high progenitor mass.

2.5 Progenitor Oxygen Mass Estimate

To further constrain the progenitor properties of SN 2022crr, we estimated the oxygen mass ($M_{\rm O}$) synthesized in the explosion using the flux of the [O I] $\lambda\lambda$6300, 6364 emission line in the nebular spectrum at +133 days. At this epoch, the supernova ejecta have become optically thin, and the [O I] emission is assumed to arise from collisional excitation and radiative de-excitation of neutral oxygen. Under these conditions, the oxygen line luminosity provides a reliable proxy for the total oxygen mass in the ejecta [e.g., Uomoto, 1986, Jerkstrand et al., 2015].

The LRIS spectrum was first corrected for redshift and extinction. We then performed a local continuum subtraction using a low-order polynomial and fit a Gaussian profile to the [O I] doublet feature. The total flux in the [O I] line was computed as:

$$F_{[\rm O\,I]} = A \cdot \sigma \cdot \sqrt{2\pi}, \quad (3)$$

where A and σ are the amplitude and standard deviation of the Gaussian model, respectively.

We then calculated the oxygen mass using the following relation:

$$M_{\rm O} = 10^8 \cdot F_{[\rm O\,I]} \cdot D^2_{\rm Mpc} \cdot \exp\left(\frac{2.28}{T_4}\right)\ {\rm M}_\odot, \quad (4)$$

where $D_{\rm Mpc}$ is the luminosity distance in megaparsecs, and T_4 is the temperature in units of 10^4 K. For SN 2022crr, we adopted a temperature of 4773 K ($T_4 = 0.4773$), which was interpolated from earlier epochs using a best-fit function to the blackbody temperature evolution derived from photometric observations. The interpolation method likely involved fitting an exponential, power-law, or low-order polynomial to the temporal evolution of the photospheric temperature.

Using the measured flux and temperature, we obtained:

$$M_{\rm O} = 1.99 \pm 3.72 \times 10^{-19}\ {\rm M}_\odot. \quad (5)$$

The extremely small statistical uncertainty arises from the covariance matrix of the Gaussian fit, though we caution that systematic uncertainties (e.g., temperature assumptions, line blending, and deviations from LTE) may dominate the true error budget. Nonetheless, this value places SN 2022crr within the upper range of stripped-envelope supernovae in terms of oxygen yield, consistent with expectations for a relatively massive progenitor.

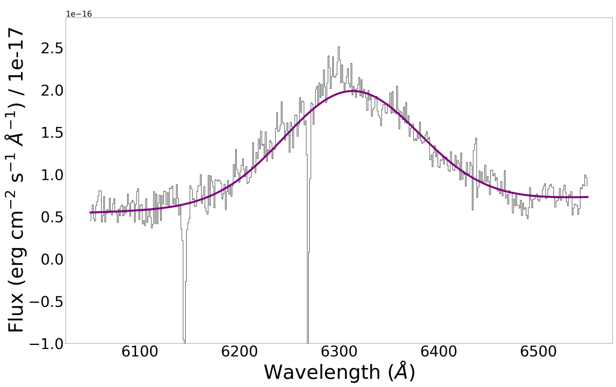

Figure 7: Gaussian fit to the [O I] $\lambda\lambda$6300, 6364 emission line in the LRIS spectrum at +133 days. The integrated line flux is used to estimate the oxygen mass of the progenitor.

Previous works have established that the mass of synthesized oxygen is a sensitive tracer of the progenitor's helium core mass and, by extension, the zero-age main sequence (ZAMS) mass. Model comparisons from nebular spectral synthesis show that SNe with oxygen masses exceeding $\sim 1\ M_\odot$ typically originate from progenitors with ZAMS masses in the range of 25–35 $M_\odot$, depending on explosion energy and fallback [Jerkstrand et al., 2015, Maeda and Nomoto, 2007, Nomoto et al., 2006]. The oxygen yield measured for SN 2022crr is therefore consistent with a massive star that underwent extensive stripping of its outer layers prior to collapse, potentially via binary interaction or strong stellar winds.

References

A. Jerkstrand, S. J. Smartt, M. Fraser, and et al. Nebular-phase spectra of supernovae ib/ic: diagnostics, explosion asymmetry, and oxygen masses. *Monthly Notices of the Royal Astronomical Society*, 448(3):2482–2502, 2015. doi: 10.1093/mnras/stv041.

A. Uomoto. Nebular-phase spectra of type ib supernovae: Oxygen masses and explosion models. *Astrophysical Journal*, 310:L35–L38, 1986. doi: 10.1086/184856.

K. Maeda and K. Nomoto. Bipolar supernova explosions: Nucleosynthesis and implications for abundances in extremely metal-poor stars. *Astrophysical Journal*, 660:504–515, 2007. doi: 10.1086/513062.

K. Nomoto, N. Tominaga, H. Umeda, C. Kobayashi, and K. Maeda. Nucleosynthesis yields of core-collapse supernovae and hypernovae, and galactic chemical evolution. *Nuclear Physics A*, 777:424–458, 2006. doi: 10.1016/j.nuclphysa.2006.05.008.

G. P. Srinivasaragavan, I. Sfaradi, J. Jencson, K. De, A. Horesh, M. M. Kasliwal, S. Tinyanont, M. Hankins, S. Schulze, M. C. B. Ashley, M. J. Graham, V. Karambelkar, R. Lau, A. A. Mahabal, A. M. Moore, E. O. Ofek, Y. Sharma, J. Sollerman, J. Soon, R. Soria, T. Travouillon, and R. Walters. Pgir 20eid (sn 2020qmp): A type iip supernova at 15.6 mpc discovered by the palomar gattini-ir survey. *Astronomy & Astrophysics*, 660:A138, 2022. doi: 10.1051/0004-6361/202142158. URL https://www.aanda.org/articles/aa/abs/2022/04/aa42158-21/aa42158-21.html.

T. A. Pritchard, K. Bensch, M. Modjaz, M. Williamson, F. Taddia, Y. Yao, P. K. Blanchard, G. C. Anupama, N. K. Chakradhari, S. Srivastav, M. Tanaka, K. Maeda, and K. Nomoto. The exotic type ic broad-lined supernova sn 2018gep: Blurring the line between supernovae and fast optical transients. *The Astrophysical Journal*, 905(2):145, 2020. doi: 10.3847/1538-4357/abc5c4. URL https://arxiv.org/abs/2008.04321.

D. K. Sahu, G. C. Anupama, N. K. Chakradhari, S. Srivastav, M. Tanaka, K. Maeda, and K. Nomoto. Broad-line type ic supernova sn 2014ad. *Monthly Notices of the Royal Astronomical Society*, 475(2):2591–2604, 2018. doi: 10.1093/mnras/stx3212. URL https://arxiv.org/abs/1801.07046.